proximity to catalyse the exchange of GTP for GDP, resulting in the activation of TC10.

How does TC10 affect glucose transport? Our data lead us to speculate that TC10 may mediate the activation of two separate downstream pathways by insulin. Insulin-activated TC10 might directly produce a cytoskeletal rearrangement to facilitate the exocytosis of GLUT4. Evidence suggests that actin filaments may have a crucial role in the exocytotic recruitment of GLUT4 to the plasma membrane from an intracellular pool in isolated adipocytes[25]. Alternatively, TC10 might be crucial in the regulation of GLUT4 docking and fusion with the plasma membrane. Insulin can modulate the binding of the vesicle-SNARE protein VAMP2 with the target-SNARE syntaxin 4 to control the docking and fusion of GLUT4 vesicles through a PI(3)K-independent pathway. Thus, it is tempting to speculate that the activation of TC10 is directly upstream of this event. Future studies will be needed to address these possibilities. □

Methods

Transfection of CHO/IR and 3T3L1 adipocytes

CHO/IR cells and differentiated 3T3L1 adipocytes were transiently transfected as described[1,10].

Guanine nucleotide exchange assay

We transfected 293T cells with Myc–C3G or Flag–SOS plasmid DNA. Transfected cells were cultured for 48 h, gathered and lysed in 25 mM HEPES pH 7.4, 150 mM NaCl, 1.5 mM $MgCl_2$, 0.5% Triton X-100 and protease inhibitors. Myc–C3G and Flag–SOS proteins were immunoprecipitated with Myc antibody or Flag antibodies and protein-A/ G–Sepharose. Guanine nucleotide exchange assays were performed essentially as described[26]. We constructed C3G and C3GΔcdc25 by cloning the NcoI–XbaI and NcoI–SmaI fragments, respectively, of the coding sequence of C3G into a pCS2-mt vector with a 5′ Myc epitope tag.

Affinity precipitation of TC10 using GST–Pak1 PBD

We modified the method from ref. 15. Cells were incubated with binding buffer (25 mM Tris-HCl, pH 7.5, 1 mM dithiothreitol, 30 mM $MgCl_2$, 40 mM NaCl and 0.5% Nonidet P-40) in the presence of 7 μg of GST–Pak1 pzi-binding domain (PBD) agarose (Upstate) for 1 h at 4 °C. The beads were washed three times with 1% Nonidet P-40 washing buffer. The beads were suspended in sample buffer, separated by 4–20% SDS–PAGE, transferred to a nitrocellulose membrane, and blotted with anti-HA monoclonal antibody.

1. Min, J. et al. Synip: a novel insulin-regulated syntaxin 4-binding protein mediating GLUT4 translocation in adipocytes. Mol. Cell 3, 751–760 (1999).
2. Olson, A. L., Knight, J. B. & Pessin, J. E. Syntaxin 4, VAMP2, and/or VAMP3/ cellubrevin are functional target membrane and vesicle SNAP receptors for insulin-stimulated GLUT4 translocation in adipocytes. Mol. Cell. Biol. 17, 2425–2435 (1997).
3. Hausdorff, S. F., Bennett, A. M., Neel, B. G. & Birnbaum, M. J. Different signaling roles of SHPTP2 in insulin-induced GLUT1 expression and GLUT4 translocation. J. Biol. Chem. 270, 12965–12968 (1995).
4. Elmendorf, J. S., Chen, D. & Pessin, J. E. Guanosine 5′-O-(3-thiotriphosphate) stimulation of GLUT4 translocation is tyrosine kinase-dependent. J. Biol. Chem. 273, 13289–13296 (1998).
5. Holman, G. D. et al. Cell surface labeling of glucose transporter isoform GLUT4 by bis-mannose phospholabel. Correlation with stimulation of glucose transport in rat adipose cells by insulin and phorbol ester. J. Biol. Chem. 265, 181172–18179 (1990).
6. Piper, R. C., Hess, L. J. & James, D. E. Differential sorting of two glucose transporters expressed in insulin-sensitive cells. Am. J. Physiol. 260, C570–580 (1991).
7. Pessin, J. E. & Saltiel, A. R. Signaling pathways in insulin action: molecular targets of insulin resistance. J. Clin. Invest. 106, 165–169 (2000).
8. Ribon, V. & Saltiel, A. R. Insulin stimulates tyrosine phosphorylation of the proto-oncogene product of c-Cbl in 3T3-L1 adipocytes. Biochem. J. 324, 839–845 (1997).
9. Ribon, V., Printen, J. A., Hoffman, N. G., Kay, B. K. & Saltiel, A. R. A novel, multifunctional c-Cbl binding protein in insulin receptor signaling in 3T3-L1 adipocytes. Mol. Cell. Biol. 18, 872–879 (1998).
10. Baumann, C. A. et al. CAP defines a second signaling pathway required for insulin-stimulated glucose transport. Nature 407, 202–207 (2000).
11. Aspenstrom, P. Effectors for the rho GTPases. Curr. Opin. Cell Biol. 11, 95–102 (1999).
12. Kjoller, L. & Hall, A. Signaling to rho GTPases. Exp. Cell. Res. 253, 166–179 (1999).
13. Neudauer, C. L., Joberty, G., Tatsis, N. & Macara, I. G. Distinct cellular effects and interactions of the rho-family GTPase TC10. Curr. Biol. 8, 1151–1160 (1998).
14. Jou, T. S., Schneeberger, E. E. & Nelson, W. J. Structural and functional regulation of tight junctions by rhoA and rac1 small GTPases. J. Cell Biol. 142, 101–115 (1998).
15. Benard, V., Bohl, B. P. & Bokoch, G. M. Characterization of rac and cdc42 activation in chemo-attractant-stimulated human neutrophils using a novel assay for active GTPases. J. Biol. Chem. 274, 13198–13204 (1999).
16. Owen, D., Mott, H. R., Laue, E. D. & Lowe, P. N. Residues in cdc42 that specify binding to individual CRIB effector proteins. Biochemistry 39, 1243–1250 (2000).
17. Thompson, G., Owen, D., Chalk, P. A. & Lowe, P. N. Delineation of the cdc42/rac-binding domain of p21-activated kinase. Biochemistry 37, 7885–7891 (1998).
18. Wiese, R. J., Mastick, C. C., Lazar, D. F. & Saltiel, A. R. Activation of mitogen-activated protein kinase and PI 3-kinase is not sufficient for the hormonal stimulation of glucose uptake, lipogenesis, or glycogen synthesis in 3T3-L1 adipocytes. J. Biol. Chem. 270, 3442–3446 (1995).
19. Isakoff, S. J. et al. The inability of PI 3-kinase activation to stimulate GLUT4 translocation indicates additional signaling pathways are required for insulin-stimulated glucose uptake. Proc. Natl Acad. Sci. USA 92, 10247–10251 (1995).
20. Guilherme, A. and Czech, M. P. Stimulation of IRS-1-associated PI 3-kinase and Akt/ protein kinase B but not glucose transport by beta 1 integrin signaling in rat adipocytes. J. Biol. Chem. 273, 33119–33122 (1998).
21. Okada, T., Kawano, Y., Sakakibara, T., Hazeki, O. & Ui, M. Essential role of PI 3-kinase in insulin-induced glucose transport and antilipolysis in rat adipocytes. Studies with a selective inhibitor wortmannin. J. Biol. Chem. 269, 3568–3573 (1994).
22. Madge, L. A. & Pober, J. S. A PI-3 kinase/Akt pathway, activated by TNF or IL-1 inhibits apoptosis but not activate NF kappa B in human endothelial cells. J. Biol. Chem. 275, 15458–15465 (2000).
23. Knudsen, B. S., Feller, S. M. & Hanafusa, H. Four proline-rich sequences of the guanine-nucleotide exchange factor C3G bind with unique specificity to the first Src homology 3 domain of crk. J. Biol. Chem. 269, 32781–32787 (1994).
24. Gotoh, T. et al. Identification of Rap1 as a target for the crk SH3 domain binding guanine nucleotide-releasing factor C3G. Mol. Cell. Biol. 15, 6746–6753 (1995).
25. Omata, W., Shibata, H. Kuniaki, L. L. & Kojima, I. Actin filaments play a critical role in insulin-induced exocytotic recruitment but not in endocytosis of GLUT4 in isoleated rat adipocytes. Biochem. J. 346, 321–328 (2000).
26. Horii, Y., Beeler, J. F., Sakaguchi, M., Tachibana, M. & Miki, T. A novel oncogene, ost, encodes a guanine nucleotide exchange factor that potentially links Rho and Rac signaling pathways. EMBO J. 13, 4776–4786 (1994).
27. Thurmond, D. C., Kanzaki, M, Khan, A. H. & Pessin, J. E. Munc18c function is required for insulin-stimulated plasma membrane fusion of GLUT4 and insulin-responsive amino peptidase storage vesicles. Mol. Cell. Biol. 20, 379–388 (2000).

....

The neuronal repellent Slit inhibits leukocyte chemotaxis induced by chemotactic factors

Jane Y. Wu*, Lili Feng†, Hwan-Tae Park*, Necat Havlioglu*, Leng Wen‡, Hao Tang*, Kevin B. Bacon§, Zhi-hong Jiang*, Xiao-chun Zhang* & Yi Rao‡

* Departments of Pediatrics, and Molecular Biology and Pharmacology, and
‡ Department of Anatomy and Neurobiology, Washington University School of Medicine, Box 8108, 660 S. Euclid Avenue, St Louis, Missouri 63110, USA
† Department of Medicine, Division of Nephrology, Baylor College of Medicine, One Baylor Plaza, N730 Houston, Texas 77030, USA
§ Department of Biology I, Bayer Yakuhin Ltd, 6-5-1-3 Kunimidai, Kizu-cho, Soraku-gun, Kyoto, Japan

....

Migration is a basic feature of many cell types in a wide range of species[1]. Since the 1800s, cell migration has been proposed to occur in the nervous and immune systems[2,3], and distinct molecular cues for mammalian neurons and leukocytes have been identified. Here we report that Slit, a secreted protein previously known for its role of repulsion in axon guidance and neuronal migration, can also inhibit leukocyte chemotaxis induced by chemotactic factors. Slit inhibition of the chemokine-induced chemotaxis can be reconstituted by the co-expression of a chemokine receptor containing seven transmembrane domains and Roundabout (Robo), a Slit receptor containing a single transmembrane domain. Thus, there is a functional interaction between single and seven transmembrane receptors. Our results reveal the activity of a neuronal guidance cue in regulating leukocyte migration and indicate that there may be a general

conservation of guidance mechanisms underlying metazoan cell migration. In addition, we have uncovered an inhibitor of leukocyte chemotaxis, and propose a new therapeutic approach to treat diseases involving leukocyte migration and chemotactic factors.

Leukocyte chemotaxis is one of the best-characterized models of cell migration in adult mammals[4–12]. Work in the past 20 years has demonstrated the importance of the chemokine family in leukocyte chemotaxis[4–9]. These structurally related small proteins regulate leukocyte migration and function[4–9]. Neuronal migration is an important step in neural development in the nervous system[10–12]; however, it is not clear whether mechanisms operating in the nervous system are conserved in the immune system. Leukocytes migrate at a rate much faster than neurons: the behaviour of leukocytes can be monitored in seconds, whereas that of the neurons is monitored in tens of minutes and hours. The cellular environment in which leukocytes migrate also seems to be different from that for axons and neurons. The morphology of migrating neurons, which have a rather long leading process, differs from that of leukocytes. At the molecular level, all neuronal guidance cues

bind to receptors containing a single transmembrane domain. By contrast, G-protein-coupled receptors (GPCRs) containing seven transmembrane domains are thought to be the sole receptors mediating responses not only to all chemokines, but also to other chemotactic factors either for leukocytes[5] or for the social amoebae *Dictyostelium*[1]. It is therefore not obvious whether neuronal guidance cues can have roles in the haematopoietic or immune systems.

Studies on the *slit* gene family[13,14] have shown that secreted Slit proteins can guide both axon projection[15–18] and neuronal migration[19–22]. We previously observed embryonic expression of Slit and Robo outside the mammalian nervous system[17,22], which led us to speculate potential roles for Slit in several systems including the immune system[19,20]. Previous studies by us and others have focused on embryonic expression of *slit* and *robo*. We have now used RNase protection assays to examine the expression of three known *slit* genes in adult tissues and cell lines (Fig. 1a−c). Each *slit* gene has a distinct expression pattern: *slit1* is specific to the brain, but *slit2* and *slit3* are expressed in the brain as well as other tissues. The expression level of *slit2* in the kidney and the lung is comparable to that in the brain. Expression of *slit3* is the highest in the lung and
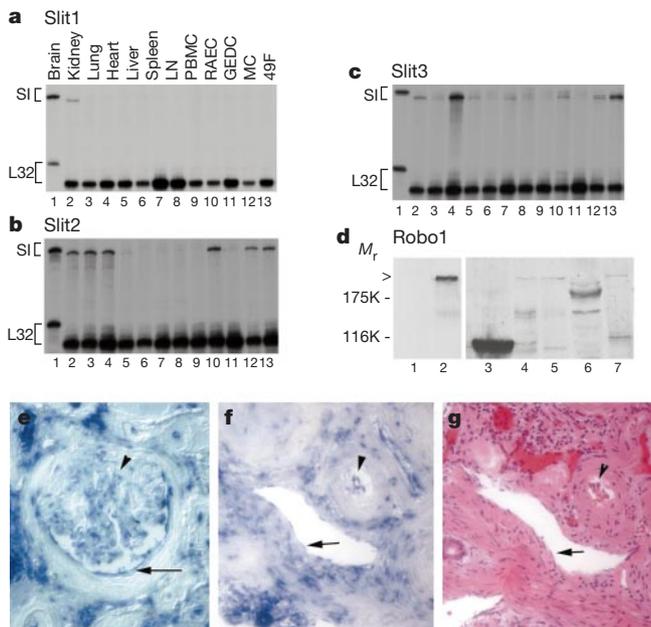

Figure 1 Expression of Slit and Robo in adult tissues. **a**−**c**, RNase protection assays (RPAs) were used to determine the expression of three *slit* genes in adult rats. Total RNA was prepared from different rat tissues and cell lines, as indicated (lanes 2−13). Total RNA (5 μg) was used in RPAs with probes specific for *slit1*, *slit2* and *slit3* genes (SI). The rat L32 gene probe controlled for RNA input (lower band in each panel). Probes in lane 1 contain polylinker regions and are longer than the protected bands. LN, lymph node; PBMC, peripheral blood mononuclear cells; RAEC, rat endothelial cell line; GEDC, glomerular endothelial cells from the rat kidney; MC, rat kidney mesangial cells; 49F, rat kidney fibroblasts. **d**, Expression of Robo1 protein detected with anti-Robo1 antibodies. Arrowhead indicates full-length Robo1. Lane 1, HEK cells; lane 2, Robo1-transfected HEK cells; lane 3, a strong band with lower relative molecular mass (M_r) than full-length Robo1 was detected reproducibly in rat thymus, indicating a crossreacting band or a proteolytically cleaved product; lane 4, HL-60 cells; lane 5, neutrophils differentiated from HL-60 cells; lane 6, rat PBMCs: no full-length Robo1 was detected but several lower M_r bands were visible; lane 7, rat lymph node. **e**, *slit2* messenger RNA distribution detected by *in situ* hybridization in the glomerulus of adult human kidney. Arrowhead indicates mesangial cells; arrow indicates epithelial cells in Bowman's capsule. In the glomerulus, most of the positive cells are epithelial cells, but some endothelial cells can be seen. **f**, *slit2* mRNA expression in vascular endothelial cells in the human kidney. Arrow indicates endothelial cells in a venule; arrowhead indicates endothelial cells in an arteriole. **g**, Haemotoxylin−eosin staining of a section of the same kidney as that shown in **f**. These two sections are not immediately next to each other, but corresponding regions are conveniently identified by landmarks in the sections.
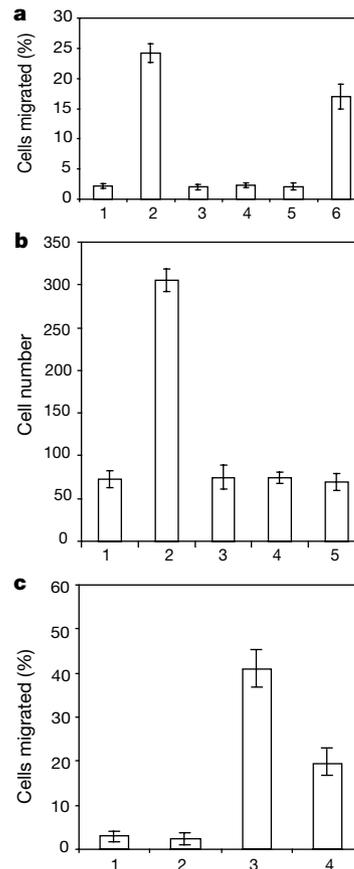

Figure 2 Effect of Slit on leukocyte chemotaxis induced by SDF-1α. **a**, Transwell migration of rat lymphocytes. Control or SDF-containing media were added to the lower chamber. Cells that migrated to the lower chamber were counted, and are expressed as a percentage of the cells added to the upper chamber. 1, control; 2, 10 nM SDF-1α; 3, 100 pM SLIT2; 4, 10 pM SLIT2; 5, 10 nM of SDF-1α and 100 pM of SLIT2; 6, 10 nM of SDF-1α and 10 pM of SLIT2. **b**, Rat lymphocytes were examined in transfilter assays in the presence of SDF-1α (10 nM). SLIT2 (100 pM) was added to the lower chamber, the upper chamber or both upper and lower chambers. 1, control; 2, SDF-1α; 3, both SDF-1α and SLIT2 in the lower chamber; 4, SDF-1α in the lower chamber and SLIT2 in the upper chamber; 5, SDF-1α in the lower chamber and SLIT2 in both chambers. **c**, Slit inhibition of chemotaxis induced by fMLP. HL-60 cells differentiated into neutrophil-like cells after treatment with DMSO. Chemotaxis was observed in transwell assays. 1, control; 2, SLIT2; 3, fMLP; 4, SLIT2 and fMLP.

also detectable in the kidney, the brain, the heart, the spleen and the lymph nodes. When a number of cell lines were examined, *slit2* and *slit3* were found in the rat endothelial cells, mesangial cells and fibroblasts from the rat kidney. *In situ* hybridization of human kidneys revealed the expression of *slit2* in mesangial and epithelial cells in the glomeruli; in epithelial cells in the tubules (Fig. 1e); and in endothelial cells of both arterioles and venules in the kidney (Fig. 1f).

Anti-Robo1 antibodies detected Robo1 in the lymph nodes, the thymus and neutrophils differentiated from HL-60 cells (Fig. 1d). By polymerase chain reaction with reverse transcription (RT–PCR), *robo1* was detected in the thymus, the spleen, the lymph nodes, the liver, the kidney and the heart (data not shown), whereas *robo2* was found in the spleen, the thymus, the liver, the lung and the kidney (data not shown).

To investigate whether Slit could affect chemotaxis, we used standard transwell and transfilter assays in which a chemokine was placed in the lower chamber and the leukocytes were placed in the upper chamber. We then analysed the migration of leukocytes into the lower chamber or onto the underside of the filter. Conditioned serum-free media from human embryonic kidney (HEK) cells expressing human and *Xenopus* Slit2 (SLIT2 and *Xenopus* Slit2) proteins[17], as well as SLIT2 and *Xenopus* Slit2 proteins purified from serum-containing conditioned media, were tested.

As expected, the chemokine stromal-derived factor (SDF)-1 induced leukocyte chemotaxis (Fig. 2a, b). Lymphocytes isolated from the lymph nodes were chemotactic towards 10 nM of SDF-1 (Fig. 2a), but chemotaxis induced by SDF-1 was reduced by the presence of 100 pM of SLIT2 in the lower chamber (Fig. 2a). This effect was dose dependent; 10 pM of SLIT2 was not effective in reducing chemotaxis induced by SDF-1 (Fig. 2a). The effect of SLIT2 in the lower chamber might be due to either repulsion or inhibition. To test whether Slit could inhibit leukocyte chemotaxis, we added SLIT2 to either the upper or the lower chamber, and SDF-1 to the lower chamber (Fig. 2b). Slit reduced SDF-1-induced chemotaxis when it was present in the upper chamber, and even when it was present in both the upper and the lower chambers. These results indicate that Slit inhibits chemotaxis induced by SDF-1.

To test whether Slit could affect chemotaxis induced by other chemotactic factors, we used the bacterial product *N*-formyl peptide f-Met-Leu-Phe (fMLP). fMLP attracts neutrophil-like cells differentiated from HL-60 cells[23]. We found that SLIT2 could inhibit the migration of differentiated HL-60 cells induced by fMLP (Fig. 2c).

Robo is a protein with a single transmembrane domain[24,25], serving as a Slit receptor in axon guidance[15–17] and neuronal migration[19,21]. To investigate whether Robo mediates leukocyte responses to Slit, we used RoboN, a fragment of Robo that contains only the extracellular part of the Robo protein[19]. The addition of RoboN abolished the inhibitory effect of Slit on leukocyte chemotaxis (Fig. 3a). Together with the expression of Robo in the haematopoietic system, these results provide evidence for the involvement of Robo in mediating Slit responses in leukocytes, supporting a conserved guidance mechanism for cell migration.

The receptor for SDF-1 is CXCR4, a GPCR with seven transmembrane domains. To determine whether Robo and CXCR4 are sufficient to mediate the functional interaction between Slit and SDF-1, we introduced Robo and CXCR4 separately or together into HEK cells (Fig. 3b). When transfected with CXCR4, HEK cells migrated towards SDF-1. However, Slit significantly reduced SDF-1-induced chemotaxis of HEK cells expressing both *robo1* and CXCR4, showing that the functional interaction between Slit and
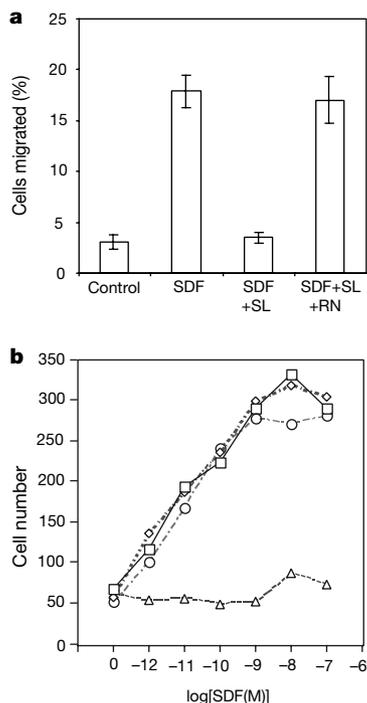
Figure 3 Robo is involved in mediating Slit inhibition of chemotaxis. **a**, The effect of Slit is inhibited by RoboN. Chemotaxis was analysed by using rat lymph node cells in transwell assays. SLIT2 (SL) and RoboN (RN) were added to the upper well and SDF-1α was added to the lower well. **b**, Expression of CXCR4 and Robo in HEK cells can reconstitute Slit inhibition of SDF-1α-induced chemotaxis. HEK migration was measured with the transfilter assay in microchemotaxis chambers using HEK cells expressing CXCR4, or both CXCR4 and rat Robo1 in the presence of different concentrations of SDF-1α. Control vehicle or 100 pM of purified Slit protein was added. Squares, migration of HEK cells expressing CXCR4 in response to SDF-1; diamonds, migration of HEK cells expressing CXCR4 in response to SDF-1α in the presence of Slit; circles, migration of HEK cells expressing Robo and CXCR4 in response to SDF-1α; triangles, migration of HEK cells expressing Robo and CXCR4 in response to SDF-1α in the presence of Slit.
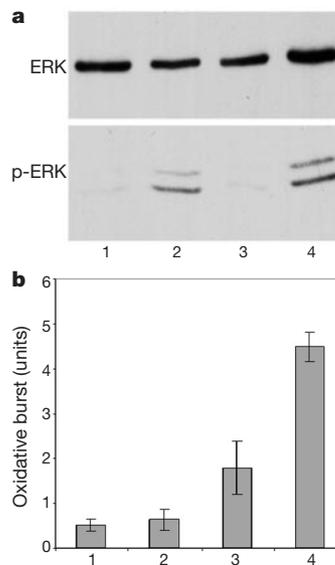
Figure 4 Lack of general inhibition by Slit. **a**, Neutrophils differentiated from HL-60 were treated with fMLP, or fMLP and SLIT2. Phosphorylation of ERK was examined by an anti-phospho-ERK antibody. Top, anti-ERK staining; bottom, anti-phospho-ERK staining. fMLP could induce ERK phosphorylation, which was not inhibited by the addition of SLIT2. Lane 1, control; lane 2, fMLP; lane 3, SLIT2; lane 4, fMLP and SLIT2. **b**, Oxidative burst was shown by SOD-inhibitable production of superoxide, and 1 unit was defined as nmol per 2×10^6 cells per 15 min. 1, control; 2, SLIT2; 3, fMLP; 4, SLIT 2 and fMLP. Results shown are representative of three experiments, each with triplicate samples.

the chemokine SDF-1 could be reconstituted in HEK cells by the expression of both Robo and CXCR4.

We next considered whether the inhibitory effect of Slit on migratory responses was due to a general inhibitory or toxic effect on leukocytes. We tested whether Slit could inhibit two activities of fMLP that are not related to cell migration. fMLP activates the extracellular signal-regulated kinases 1 and 2 (ERK1 and ERK2) by causing their phosphorylation (Fig. 4a)[26,27]; however, Slit did not inhibit fMLP-induced ERK phosphorylation (Fig. 4a). fMLP also causes the oxidative burst of neutrophils[28] (Fig. 4b); Slit did not cause oxidative burst, nor did it inhibit the oxidative burst induced by fMLP (Fig. 4b). In fact, Slit increased the oxidative burst induced by fMLP, which is consistent with the previous observation that regulation of the actin cytoskeleton can prime cells for oxidative burst. These results indicate that Slit inhibits chemotaxis, but not all other functions of leukocytes.

Our findings that Slit can inhibit chemotaxis of leukocytes induced by chemotactic factors have implications in the conservation of molecular mechanisms of cell migration between species, and in biological and therapeutic regulations of immune responses and other physiological or pathological processes involving chemotactic factors. We suggest that neuronal guidance cues such as netrins, semaphorins and ephrins may also guide leukocyte migration and regulate biological processes involving chemotactic factors. Other molecules involved in neuronal positioning, such as Reelin[12], should also be tested for their potential roles in leukocyte migration. Our results in HEK cells indicate a functional interaction between the single transmembrane receptor Robo and the GPCRs, suggesting a mechanism for regulating signal transduction pathways mediated by GPCRs and heterotrimeric G proteins.

Past research in leukocyte chemotaxis has been focused mainly on chemoattractants and positive regulation. Although there were reports of virally produced inhibitors of chemokines[29,30], there is no known endogenous negative factors. Our results reveal that there are negative regulators of leukocyte chemotaxis available endogenously, which may be important in physiological and pathological situations. This expands the scope and the perspective of research in leukocyte biology. Chemokines have several roles, including inflammatory responses, leukocyte activation, lymphocyte trafficking and lymphoid organ homeostasis, tissue injury, haematopoiesis, atherosclerosis, allogeneic transplant rejection, angiogenesis, virally induced vascular diseases, cardic morphogenesis, and tumour development. In all of these situations except tumoriogenesis, inhibition of chemokine signalling is therapeutically beneficial, and much effort has been directed towards obtaining reagents that can block chemokines or their receptors. Potential applications of Slit should be tested.

Our studies of Slit broaden the search for chemokine inhibitors. Because the inhibition of receptor signalling can block HIV infection, Slit inhibition of chemokine receptors including CXCR4 (and CCR5; data not shown) suggests that Slit cannot be ruled out as a useful reagent in inhibiting HIV infection; thus, the therapeutic potentials for Slit and other negative factors are an attractive area of further research. Our unpublished data indicate that *in vivo* application of Slit protein attenuates crescentic glomerulonephritis in an animal model involving chemokine-induced leukocyte infiltration. In summary, our findings of Slit inhibition of leukocyte chemotaxis induced by chemotactic factors not only shed light on the fundamental conservation of mechanisms guiding cell migration, but also open up new areas for future investigations. □

Methods

RNase protection assay

We used 5 μg total RNA for each sample prepared from tissues or cultured cells in RNase protection assays. Riboprobes specific for rat *slit1*, *slit2* and *slit3* genes were prepared, and RNase protection assay was performed using a kit (Torrey Pines Biologicals) according to the manufacturer's protocols with corresponding probes labelled with [^{32}P]UTP.

Isolation of leukocytes and assays with HL-60 cells

Leukocytes were isolated from rat lymph nodes, spleen or peripheral blood according to standard protocols. Cells were kept at 4 °C in media containing 5% fetal calf serum (FCS) until use; and cells were used within 8 h after isolation.

We grew the HL-60 cell line under standard conditions with RPMI-1640 media supplemented with 10% heat-inactivated FCS[23]. Cells induced with 1.2% dimethyl sulphoxide (DMSO) were obtained by seeding HL-60 cells at 3×10^6 ml^{-1} in growth media and culturing for 4–6 days (ref. 23). ERK Phosphorylation induced by 1 min of fMLP stimulation was examined with anti-phospho ERK antibody[26]. In Fig. 4a, serum-free conditioned medium from control HEK cells was used as control in lane 1; 100 nM of fMLP in the presence of serum-free conditioned medium from control HEK cells was used in lane 2; serum-free conditioned medium from SLIT2-secreting HEK cells was used in lane 3; 100 nM of fMLP in the presence of serum-free conditioned medium from SLIT2 secreting HEK cells was used in lane 4. In Fig. 4b, oxidative burst was quantified according as described[28] by measuring the superoxide dismutase (SOD)-inhibitable reduction of cytochrome *c*. Briefly, differentiated HL-60 cells (2×10^6) containing 75 μM cytochrome *c* with or without SOD (30 μg) were incubated with fMLP (100 nM) for 15 min at 37 °C. The reaction was stopped by submerging the tubes in ice. The tubes were centrifuged, and the absorbency of the supernatant at 550 nM was measured in a spectrophotometer.

Assays for leukocyte chemotaxis

Leukocyte chemotaxis was measured by transwell and transfilter assays. Isolated leukocytes were resuspended at a concentration of 4×10^6 cells per ml in 50% DMEM, 50% M199, 5% heat-inactivated fetal bovine serum (FBS). Unless otherwise specified, 10 nM chemokines were placed at lower wells of chemotaxis chambers. Chemotaxis results are representative of at least three independent experiments performed in triplicates.

In the transwell assay, cells (100 μl) were put in inserts (5 μm in pore size) (Costar) placed in 24-well dish containing 600 μl of culture media per well with a chemokine or the Slit protein. After incubation at 37 °C for 1.5–3 h, cells migrated through the insert filter into the lower well were collected and counted.

In the transfilter assay, we placed different chemokines and Slit in the lower wells of a 48-well chemotaxis chamber (Neuroprobe, Cabin John, MD) and separated them by a polyvinylpyrolidone-free polycarbonate filter (5 or 8 μm in pore size). Isolated leukocytes or transfected HEK cells (50 μl) were put in the upper wells. After incubating at 37 °C for 2 h, cells on the top surface of the filter were removed and cells that had migrated through the filter onto the undersurface were fixed in methanol and stained. We expressed the transfilter migration of cells as cell number for five high-power (×400) fields.

HEK cell culture

We grew HEK cells in DMEM supplemented with 10% FBS. An HEK cell line expressing the extracellular domain of rat Robo1 protein tagged at the carboxy terminus with an haemagglutinin A (HA) tag (RoboN)[19] was cultured in DMEM and 5% FBS. The RoboN-containing media was collected 3–4 d after cells became confluent. The RoboN-containing media was diluted to roughly 1 nM and used in cell migration assay. We also established a stable HEK cell line expressing rat CXCR4.

1. Devreotes, P. N. & Zigmond, S. H. Chemotaxis in eukaryotic cells: a focus on leukocytes and *Dictyostelium*. *Annu. Rev. Cell Biol.* **4,** 649–686 (1988).
2. McCutcheon, M. Chemotaxis in leukocytes. *Physiol. Rev.* **26,** 319–336 (1946).
3. Bentivoglio, M. & Mazzarello, P. The history of radial glia. *Brain Res. Bull.* **49,** 305–315 (1999).
4. Springer, T. A. Traffic signals for lymphocyte recirculation and leukocyte emigration: the multistep paradigm. *Cell* **76,** 301–314 (1994).
5. Murphy, P. M. The molecular biology of leukocyte chemoattractant receptors. *Annu. Rev. Immunol.* **12,** 593–633 (1994).
6. Baggiolini, M. Chemokines and leukocyte traffic. *Nature* **392,** 565–568 (1998).
7. Luster, A. D. Chemokines—chemotactic cytokines that mediate inflammation. *N. Engl. J. Med.* **338,** 436–445 (1998).
8. Cyster, J. G. Chemokines and cell migration in secondary lymphoid organs. *Science* **286,** 2098–2102 (1999).
9. Campbell, J. J. & Butcher, E. C. Chemokines in tissue-specific and microenvironment-specific lymphocyte homing. *Curr. Opin. Immunol.* **12,** 336–341 (2000).
10. Rakic, P. Principles of neural cell migration. *Experientia* **46,** 882–891 (1990).
11. Hatten, M. E. & Heintz, N. in *Fundamentals of Neuroscience* (ed. Zigmond, M.) 451–479 (Academic, New York, 1998).
12. Rice, D. S. & Curran, T. Mutant mice with scrambled brains: understanding the signaling pathways that control cell positioning in the CNS. *Genes Dev.* **13,** 2758–2773 (1999).
13. Nusslein-Volhard, C., Wieschaus, E. & Kluding, H. Mutations affecting the pattern of the larval cuticle in *Drosophila melanogaster*. I. Zygotic loci on the second chromosome. *Roux's Arch. Dev. Biol.* **193,** 267–282 (1984).
14. Rothberg, J. M., Hartley, D. A. Walther, Z. & Artavanis-Tsakonas, S. *slit*: an EGF-homologous locus of *D. melanogaster* involved in the development of the embryonic central nervous system. *Cell* **55,** 1047–1059 (1988).
15. Kidd, T., Bland, K. S. & Goodman, C. S. Slit is the midline repellent for the Robo receptor in *Drosophila*. *Cell* **96,** 785–794 (1999).
16. Brose, K. *et al.* Evolutionary conservation of the repulsive axon guidance function of Slit proteins and of their interactions with Robo receptors. *Cell* **96,** 795–806 (1999).
17. Li, H. S. *et al.* Vertebrate Slit, a secreted ligand for the transmembrane protein roundabout, is a repellent for olfactory bulb axons. *Cell* **96,** 807–818 (1999).
18. Wang, K. H. *et al.* Purification of an axon elongation- and branch-promoting activity from brain identifies a mammalian Slit protein as a positive regulator of sensory axon growth. *Cell* **96,** 771–784 (1999).

951

19. Wu, W. et al. Directional guidance of neuronal migration in the olfactory system by the secreted protein Slit. Nature 400, 331–336 (1999).
20. Hu, H. Chemorepulsion of neuronal migration by Slit2 in the developing mammalian forebrain. Neuron 23, 703–711 (1999).
21. Zhu, Y., Li, H. S., Zhou, L., Wu, J. Y. & Rao, Y. Cellular and molecular guidance of GABAergic neuronal migration from the striatum to the neocortex. Neuron 23, 473–485 (1999).
22. Yuan, W. et al. The mouse Slit family: secreted ligands for Robo expressed in patterns that suggest a role in morphogenesis and axon guidance. Dev. Biol. 212, 290–306 (1999).
23. Collins, S. J., Fuscetti, F. W., Gallagher, R. E. & Gallo, R. C. Normal functional characteristics of cultured human promyelocytic leukemia cells (HL60) after induction of differentiation by dimethylsulfoxide. J. Exp. Med. 149, 969–974 (1979).
24. Kidd, T. et al. Roundabout controls axon crossing of the CNS midline and defines a novel subfamily of evolutionarily conserved guidance receptors. Cell 92, 205–215 (1998).
25. Zallen, J. A., Yi, B. A. & Bargmann, C. I. The conserved immunoglobulin superfamily member SAX-3/Robo directs multiple aspects of axon guidance in C. elegans. Cell 92, 217–227 (1998).
26. Krump, E., Sanghera, J. S., Pelech, S. L., Furuya, W. & Grinstein, S. Chemotactic peptide N-formyl-Met-Leu-Phe activation of p38 mitogen-activated protein kinase (MAPK) and MAPK-activated protein kinase-2 in human neutrophils. J. Biol. Chem. 272, 937–944 (1997).
27. Downey, G. P. et al. Importance of Mek in neutrophil microbicidal responsiveness. J. Immunol. 160, 434–443 (1998).
28. O'Brien, P. J. Superoxide production. Methods Enzymol. 105, 370–379 (1984).
29. Smith, C. A. et al. Poxvirus genomes encode a secreted, soluble protein that preferentially inhibits beta chemokine activity yet lacks sequence homology to known chemokine receptors. Virology 236, 316–327 (1997).
30. Kledal, T. N. et al. A broad-spectrum chemokine antagonist encoded by Kaposi's sarcoma-associated herpes virus. Science 277, 1656–1659 (1997).

....

Phototropin-related NPL1 controls chloroplast relocation induced by blue light

Jose A. Jarillo*, Halina Gabrys†, Juan Capel*‡, Jose M. Alonso*§, Joseph R. Ecker*§ & Anthony R. Cashmore*

* Plant Science Institute, Department of Biology, University of Pennsylvania, Philadelphia, Pennsylvania 19104-6018, USA
† Institute of Molecular Biology, Jagiellonian University, 31-120 Krakow, Poland
‡ Departamento de Biología Aplicada, Universidad de Almería, 04120 Almeria, Spain

....

In photosynthetic cells, chloroplasts migrate towards illuminated sites to optimize photosynthesis and move away from excessively illuminated areas to protect the photosynthetic machinery[1]. Although this movement of chloroplasts in response to light has been known for over a century, the photoreceptor mediating this process has not been identified. The Arabidopsis gene NPL1 (ref. 2) is a paralogue of the NPH1 gene, which encodes phototropin, a photoreceptor for phototropic bending[3]. Here we show that NPL1 is required for chloroplast relocation induced by blue light. A loss-of-function npl1 mutant showed no chloroplast avoidance response in strong blue light, whereas the accumulation of chloroplasts in weak light was normal. These results indicate that NPL1 may function as a photoreceptor mediating chloroplast relocation.

§ Present address: Plant Biology Laboratory, The Salk Institute for Biological Studies, La Jolla, California 92037, USA.

In most plants, chloroplast movement is controlled by blue light and is affected by light direction, as well as wavelength and irradiance[4]. When leaves are exposed to low fluence rates of light, the chloroplasts gather at the periclinal walls, perpendicular to the leaf surface, to maximize photosynthesis. Under high fluence rates of light, chloroplast damage is minimized by movement of the chloroplasts towards the anticlinal walls parallel to the leaf surface. From studies of action spectra, this response appears to involve a flavin[1], and in some cases phytochrome appears to be involved (see ref. 5 and references therein).

The NPL1 gene[2] encodes a protein that is similar in sequence to Arabidopsis NPH1 (ref. 3), as well as the oat, rice, maize and fern NPH1-related proteins[6–9] (see Supplementary Information Fig. 1). The Arabidopsis NPH1 and NPL1 proteins have overall 58% identity and 67% similarity. The amino-terminal LOV1 and LOV2 domains are highly conserved[3]. Furthermore, the cysteine residues, which are important in the photochemical reactions involving flavin mononucleotide (FMW) bound to the LOV domains of NPH1 (ref. 10), are also conserved in NPL1 and the other phototropin family members. This observation indicates that NPL1 (and the other phototropin-like proteins) may also bind FMN as a chromophore. Likewise, high similarity (almost 80%) between phototropin and NPL1 is found in the eleven kinase signature domains that constitute almost the entire carboxy-terminal part of the phototropin-like proteins[11] (see Supplementary Information Fig. 1).

To analyse the expression pattern of the NPL1 transcript, we extracted total RNA from roots, stems, leaves and flowers of Arabidopsis plants. NPL1 messenger RNA was expressed in all of these organs except roots, with the highest expression detected in leaves (Fig. 1a). Because NPL1 RNA was most abundant in green tissues, we investigated the effect of light on its expression. The expression of NPL1 mRNA increased when Arabidopsis seedlings were grown under continuous white light, ultraviolet-A or blue light (Fig. 1b). Expression of the rice gene OsNPH1b, an apparent orthologue of NPL1, is also induced by light, whereas OsNPH1a, an orthologue of NPH1, is downregulated by light[8].
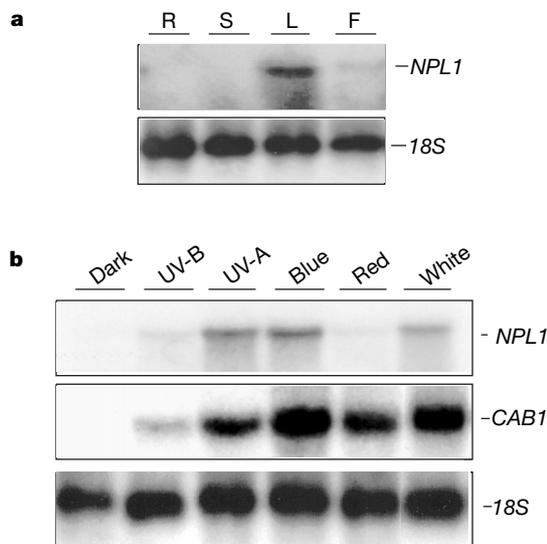
Figure 1 Tissue expression and light inducibility of NPL1 mRNA. **a**, RNA-blot hybridizations of total RNA (10 μg) extracted from roots (R), stems (S), leaves (L) and flowers (F) of 3–4-week-old plants using a NPL1 probe. **b**, Total RNA (10 μg) from 6-day-old etiolated seedlings exposed to different light treatments were fractionated by electrophoresis, blotted and hybridized with a NPL1 probe. RNA was prepared from dark-grown seedlings which were subsequently exposed to ultraviolet-B, ultraviolet-A, blue, red or white light. As a control for the light treatments, the blot was stripped and hybridized with a probe that detects CAB1 mRNA[19]. As a loading control, blots were reprobed with the 18S ribosomal RNA gene.